

Extending the Structure-Activity Relationship of Disorazole C₁: Exchanging the Oxazole Ring by Thiazole and Influence of Chiral Centers within the Disorazole Core on Cytotoxicity

Luca Lizzadro,^[a] Oliver Spieß,^[a] Wera Collisi,^[b] Marc Stadler,^[b] and Dieter Schinzer*^[a]

The synthesis of novel disorazole C₁ analogues is described and their biological activity as cytotoxic compounds is reported. Based on our convergent entry to the disorazole core we present a flexible and robust strategy to construct a variety of interesting new analogues. In particular, two regions of the molecules were examined for structural modification: 1. Replacement of the heterocyclic moiety by an exchange of the

oxazole ring by a thiazole; and 2. Evaluation of the influence of the absolute configuration of the chiral centers of the molecule. Predicated on our flexible strategy we were able to construct all analogues in an efficient way and could perform an exciting SAR (structure-activity-relationship) study to obtain insight in the cytotoxic activity influenced by the chiral centers of the disorazole core.

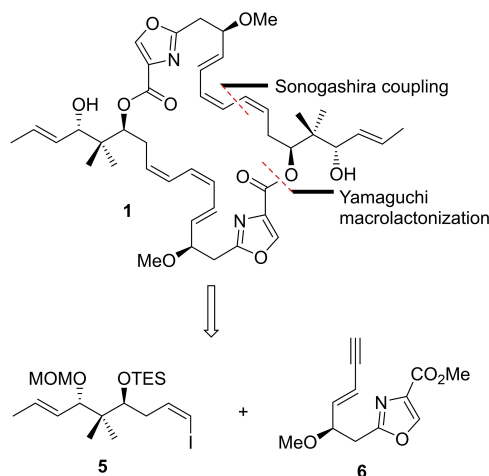
Introduction

The disorazoles represent a family of 31 macrodiolides isolated for the first time in 1994 from the fermentation broth of the myxobacterium *Sorangium cellulosum* strain So ce12,^[1] except for disorazole Z and its epoxide, which were discovered 13 years later.^[2] They show potent antitumor activity, due to the inhibition of tubulin polymerization.^[3–5]

The intriguing properties of these natural products have generated a tremendous interest, leading them to be considered as possible payloads for antibody-drug conjugates (ADCs) in targeted cancer therapy.

Our research group has recently developed a new route for the synthesis of (–)-disorazole C₁,^[6] which involved a Sonogashira coupling to construct the backbone and connect building blocks 5 and 6, and a late Boland hydrogenation^[7] to reduce the triple bonds, after a Yamaguchi macrolactonization, as depicted in Scheme 1.

Herein, we wish to report the application of our strategy to the synthesis of three new analogues of disorazole C₁, and their biological evaluation. In the last years, several analogues of the disorazoles have been synthesized by Wipf *et al.*,^[8,9] Kalesse *et al.*,^[10] and Nicolaou *et al.*,^[11,12] biological studies performed on these derivatives and on the natural members have contributed



Scheme 1. Retrosynthetic analysis of Disorazole C₁.

to the comprehension of the structure-activity relationships (SARs) of these fascinating molecules. However, not much is known about the role of the heterocyclic moiety and the configuration of the chiral centers in the biological activity. Therefore, we selected structures 2, 3 and 4 (Figure 1) as the targeted molecules, hoping to easily transfer our synthetic strategy, and maybe find new biologically active compounds to use as potential lead compounds in investigations toward targeted cancer therapy.

Results and Discussion

The first analogue we developed was compound 2, which features a thiazole motif instead of the oxazole ring. This modification was chosen in order to better understand the importance of the heterocycle in the activity of the disorazoles.

The thiazole fragment was constructed using carboxylic acid 7,^[6] which was transformed into amide 8 by reaction with ethyl

[a] L. Lizzadro, Dr. O. Spieß, Prof. Dr. D. Schinzer
Chemisches Institut
Otto-von-Guericke-Universität
Universitätsplatz 2, 39106 Magdeburg (Germany)
E-mail: dieter.schinzer@ovgu.de

[b] W. Collisi, Prof. Dr. M. Stadler
Helmholtz-Zentrum für Infektionsforschung GmbH
Inhoffenstraße 7, 38124 Braunschweig (Germany)

Supporting information for this article is available on the WWW under <https://doi.org/10.1002/cbic.202200458>

© 2022 The Authors. ChemBioChem published by Wiley-VCH GmbH. This is an open access article under the terms of the Creative Commons Attribution Non-Commercial NoDerivs License, which permits use and distribution in any medium, provided the original work is properly cited, the use is non-commercial and no modifications or adaptations are made.

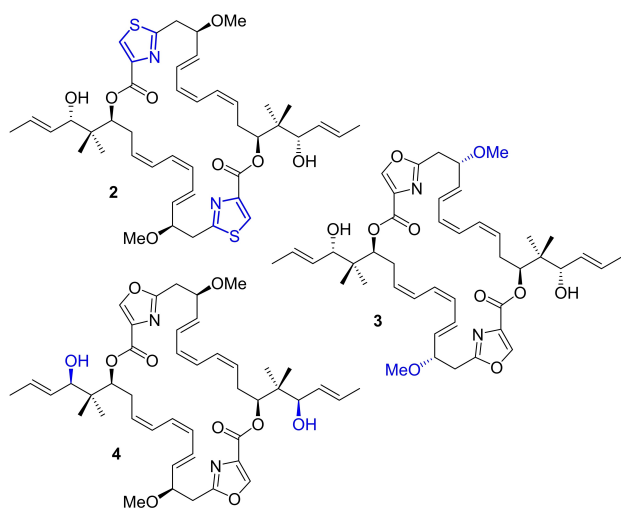
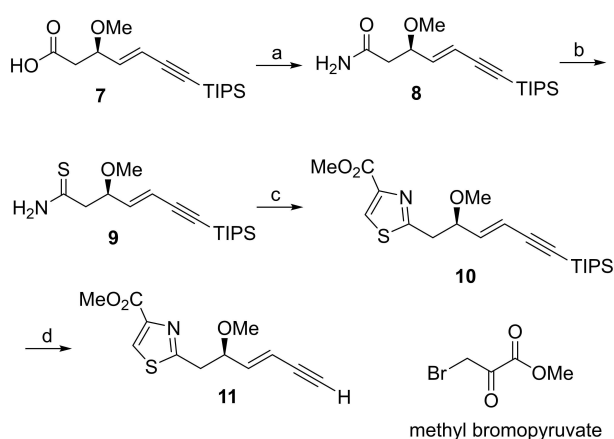


Figure 1. Structures of new Disorazole C_1 analogues.

chloroformate and subsequent treatment with aqueous NH_3 . The primary amide was converted to the corresponding thioamide **9** in 80% yield with Lawesson's reagent,^[13] and then Hantzsch's methodology^[14] was employed to build the thiazole ring. Final desilylation of the triple bond led to building block **11** in 81% yield, as depicted in Scheme 2.

The final strategy involved the coupling of fragment **11** with vinyl iodide **5**^[6] through a Sonogashira reaction, affording monomer **12**. Taking advantage of the C_2 -symmetry of the structure, we could synthesize alcohol **13** and carboxylic acid **14**, which were coupled in a Yamaguchi esterification, giving the full skeleton **15** in 77% yield. Removal of the TES group with CSA, followed by saponification and Yamaguchi macrolactonization furnished the macrocycle **16**; then final hydrogenation and deprotection of the MOM ethers with HBr delivered thiazole derivative **2**, as shown in Scheme 3.



Scheme 2. Synthesis of the Thiazole Fragment **11**. Reagents and conditions: a) ClCO_2Et , TEA, THF, 0°C , 30 min, then 25% NH_4OH , 0°C to rt, 1 h; b) Lawesson's reagent, CH_2Cl_2 , rt, 30 min, 80% (2 steps); c) methyl bromopyruvate, NaHCO_3 , THF, 0°C , 1 h, then TFAA, pyridine, -30°C , 1 h, 83%; d) TBAF, THF, 0°C to rt, 30 min, 80%. TEA = triethylamine; TFAA = trifluoroacetic anhydride; TBAF = tetra-*n*-butylammonium fluoride.

After obtaining compound **2**, we turned our attention to the chiral centers of disorazole C_1 . Therefore, we decided to change the configuration of the methoxy group-bearing chiral center next to the heterocyclic ring. To achieve this goal, we employed the same route used in the synthesis of the oxazole fragment of disorazole C_1 , which involved the enzymatic resolution of racemic β -hydroxyester **17**^[15] (Scheme 4). However, for this derivative, acetate (**S**)-**18** was taken after the reaction with Amano lipase PS instead of the (*R*)-alcohol. Deacetylation of (**S**)-**18** led to alcohol (**S**)-**17**, and subsequent methylation using trimethylxonium tetrafluoroborate furnished compound **19** in 72% yield. Ozonolysis of the olefin, followed by a Wittig reaction with ylide **21**^[16] resulted in a 2.7:1 mixture of separable *E* and *Z* isomers of the enyne **22**. The *E* isomer was treated with formic acid to give the corresponding carboxylic acid, and subsequent condensation with serine methyl ester hydrochloride delivered amide **23** in 82% yield. The usual cyclization-oxidation sequence^[6] afforded oxazole **24**, and treatment with TBAF produced the final fragment **ent-6** in 70% yield.

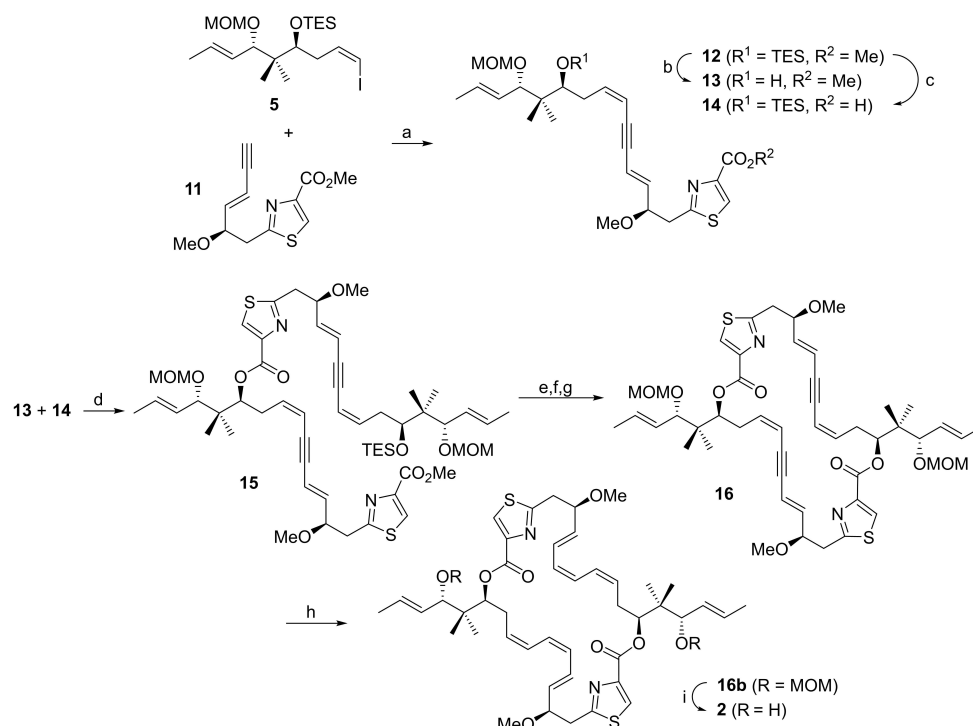
Scheme 5 summarizes the last steps of the synthesis: Sonogashira coupling between oxazole **ent-6** and vinyl iodide **5**^[6] afforded **25**. Alcohol **26** and carboxylic acid **27**, both derived from monomer **25**, were combined under Yamaguchi's conditions giving the dimer **28**. After removal of the TES group and saponification, the macrolactonization resulted in the symmetric lactone **29** in 72% yield. Finally, hydrogenation of the triple bonds and MOM deprotection delivered the desired analogue **3**.

Designing the last analogue, we envisioned that performing the allylation on aldehyde **30**^[6] using the (*S,S*)-Leighton reagent^[17] **31** instead of the (*R,R*) used in the synthesis of the natural product, we could produce the 1,3-*syn* diol **32** (Scheme 6). Interestingly, the Leighton allylation was more diastereoselective in this case (13:1 *dr*) even at room temperature. After protection of the free alcohol with MOMCl, isomerization of terminal olefin^[18] and Swern oxidation, aldehyde **34** was obtained in 77% yield, and final Stork-Zhao olefination^[19] delivered selectively the *Z*-vinyl iodide **35**.

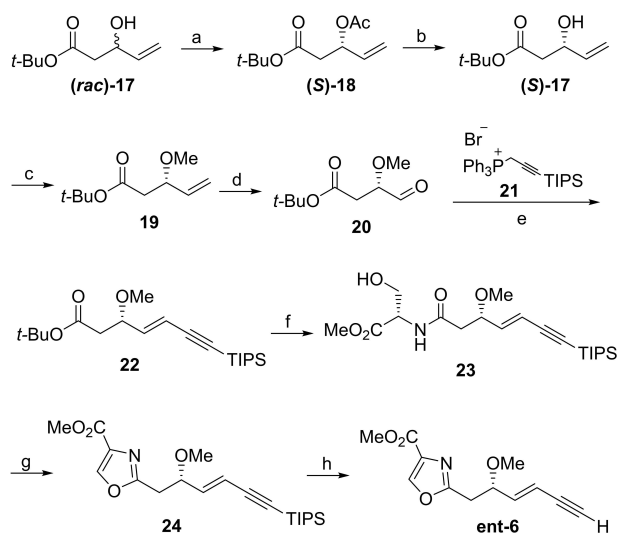
At this point, compound **35** was connected to the oxazole piece **6**^[6] in 85% yield, and the resulting monomer **36** was employed to synthesize the two key fragments for the esterification, which gave compound **39** in 75% yield. Desilylation, followed by hydrolysis of the methyl ester and macrolactonization afforded **40** in 70% yield over three steps. Boland reduction worked in 65% yield and the final analogue **4** was obtained after removal of the MOM groups, as depicted in Scheme 7.

Biological evaluation

After completing their syntheses, the biological activities of analogues **2**, **3** and **4**, along with some intermediates, were evaluated against a variety of immortalized animal and human cancer cell lines, and compared to the cytotoxicity of synthetic



Scheme 3. Total synthesis of the thiazole analogue **2**. Reagents and conditions: a) $\text{Pd}(\text{PPh}_3)_2\text{Cl}_2$, CuI , TEA , CH_3CN , -15°C to rt , 1 h, 75%; b) CSA , $\text{CH}_2\text{Cl}_2/\text{MeOH}$ 1:1, 0°C , 1 h, 95%; c) 1 M LiOH , THF , rt , 3 h, 99%; d) 1. TCBC , TEA , THF , rt , 2 h, 2. DMAP , $\text{THF}/\text{toluene}$, rt , 16 h, 77%; e) CSA , $\text{CH}_2\text{Cl}_2/\text{MeOH}$ 1:1, 0°C , 1 h; f) 1 M LiOH , THF , rt , overnight; g) 1. TCBC , TEA , THF , rt , 2 h, 2. DMAP , $\text{THF}/\text{toluene}$, rt , 16 h, 45% (3 steps); h) Zn (Ag/Cu), $\text{MeOH}/\text{H}_2\text{O}$ 1:1, 50°C , 24 h, 61%; i) HBr , $\text{CH}_3\text{CN}/\text{H}_2\text{O}$, 0°C , 1 h, 56%. CSA = camphorsulfonic acid; TCBC = 2,6,4-trichlorobenzoyl chloride; DMAP = 4-dimethylaminopyridine.



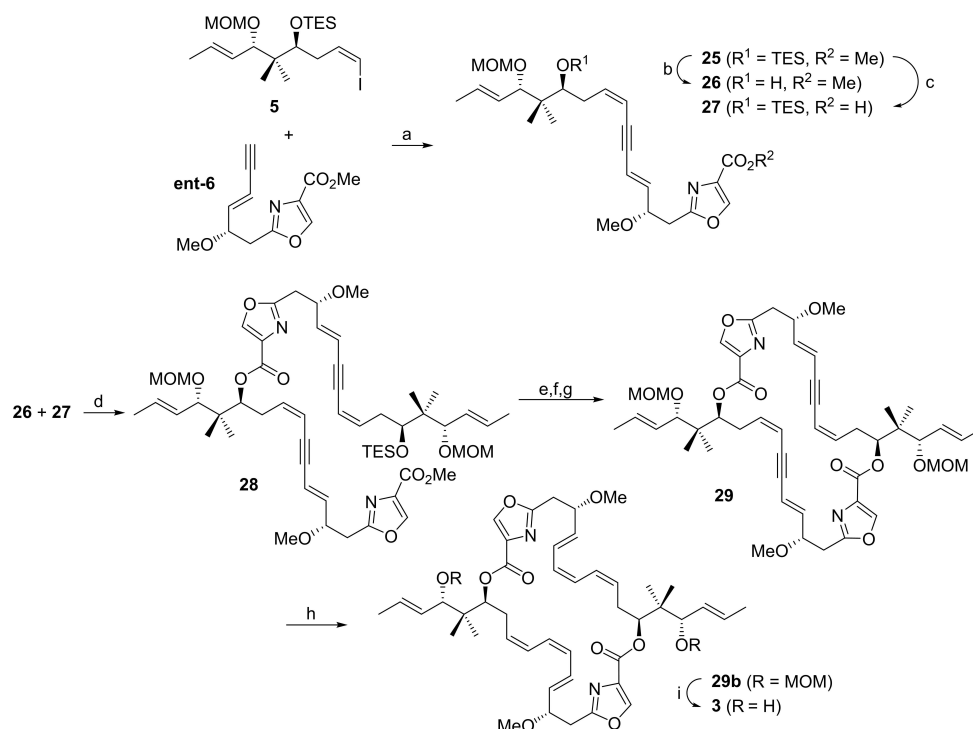
Scheme 4. Synthesis of the (*S*)-Oxazole Fragment **ent-6**. Reagents and conditions: a) Amano lipase PS , vinylacetate, 4 Å MS , pentane, 30°C , 24 h, 48%; b) K_2CO_3 , MeOH , 0°C , 30 min, 78%; c) Proton Sponge[®], Me_3OBF_4 , CH_2Cl_2 , rt , 3 h, 72%; d) O_3/O_2 , $\text{CH}_2\text{Cl}_2/\text{MeOH}$ 5:1, PPh_3 , -78°C to rt , 2 h, 92%; e) 21, $n\text{-BuLi}$, THF , 0°C to rt , 30 min, 60%; f) 1. HCOOH , rt , overnight, 2. $\text{SerOMe}\cdot\text{HCl}$, TFFH , DIPEA , THF , rt , 3 h, 82%; g) 1. DAST , K_2CO_3 , CH_2Cl_2 , -78°C to rt , 2. DBU , BrCCl_3 , CH_2Cl_2 , 0°C to rt , 16 h, 62%; h) TBAF , THF , 0°C , 30 min, 70%. $\text{SerOMe}\cdot\text{HCl}$ = serine methyl ester hydrochloride; TFFH = tetramethylfluoroformamidinium hexafluorophosphate; DIPEA = *N,N*-diisopropylethylamine; DAST = diethylaminosulfur trifluoride; DBU = 1,8-diazabicyclo[5.4.0]undec-7-ene.

disorazole C_1 . Epothilone B and disorazole A_1 were used as internal control.^[20]

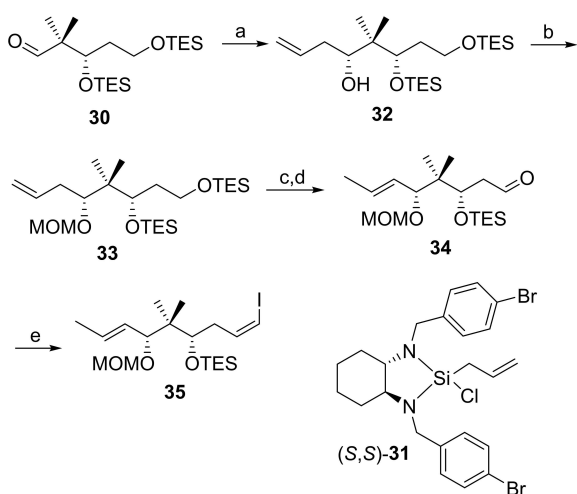
Figure 2 shows the structures of the compounds discussed below and Tables 1 and 2 summarize the results of the preliminary studies. Disorazole C_1 proved once again to be a very active compound, with IC_{50} between 0.11 and 0.60 ng/mL, only one order of magnitude less active than disorazole A_1 , as shown in Table 1.

The three derivatives exhibited lower potency than the natural product, indicating that the three-dimensional structure of the molecule is crucial in the interaction with the active site, as expected. However, analogues **2** and **3** still maintained a certain activity, showing IC_{50} in the range of nanograms/mL. On the contrary, the activity of compound **4** dropped to single digit micrograms/mL values. The lower cytotoxicity of analogue **4**, which differs from the natural product by exhibiting the opposite stereochemical orientation of the hydroxyl groups, may suggest a major involvement of this functionality in the interaction with the active site, whereas the inversion of configuration of the methoxy group-bearing chiral center in compound **3** did not lead to such a critical drop in activity. Investigation of the thiazole analogue **2** revealed that substitution of the oxazole moiety with a different heterocycle results in a slightly decreased activity.

Regarding the precursors, they were either totally inactive or less active than the corresponding final compounds, confirming the importance of the macrocyclic structure and its spatial orientation. For instance, the MOM-protected thiazole



Scheme 5. Total synthesis of analogue 3. Reagents and conditions: a) Pd(PPh₃)₂Cl₂, CuI, TEA, CH₃CN, −15 °C to rt, 75%; b) CSA, CH₂Cl₂/MeOH 1:1, 0 °C, 1 h, 97%; c) 1 M LiOH, THF, rt, 3 h, 99%; d) 1. TCBC, TEA, THF, rt, 2 h, 2. DMAP, THF/toluene, rt, 16 h, 72%; e) CSA, CH₂Cl₂/MeOH 1:1, 0 °C, 1 h; f) 1 M LiOH, THF, rt, overnight; g) 1. TCBC, TEA, THF, rt, 2 h, 2. DMAP, THF/toluene, rt, 16 h, 60% (3 steps); h) Zn (Ag/Cu), MeOH/H₂O 1:1, 50 °C, 24 h, 65%; i) HBr, CH₃CN/H₂O, −15 °C, 2.5 h, 56%.



Scheme 6. Synthesis of the vinyl iodide 35. Reagents and conditions: a) (*S,S*)-Leighton reagent 31, Sc(OTf)₃, CH₂Cl₂, rt, 24 h, 87% (13:1 dr); b) MOMCl, DIPEA, DMAP, CH₂Cl₂, reflux, overnight, 92%; c) Grubbs II cat., MeOH, 60 °C, 20 h; d) (COCl)₂, DMSO, TEA, CH₂Cl₂, −78 °C, 77% (2 steps); e) ICH₂PPh₃, NaHMDS, DMPU, THF, −78 °C, 1 h, 67%. MOMCl = methoxymethyl chloride; NaHMDS = sodium bis(trimethylsilyl)amide; DMPU = 1,3-dimethyl-3,4,5,6-tetrahydro-2(1*H*)-pyrimidinone.

analogue **16b** resulted approximately 100 times less effective than the final diol. Even the mono-protected **MOM-3** (Table 2, entry 1), derived from partial deprotection of **29** and featuring only one free alcohol with the other OH still protected

as MOM ether, showed a dramatic reduction of the activity, indicating that both alcohol functionalities are pivotal for the potency. Interestingly, the open form **15b** proved to be more active than the corresponding macrocycle **16**, probably because of the presence of the free alcohol or the carboxylic acid, which may interact with the active site.

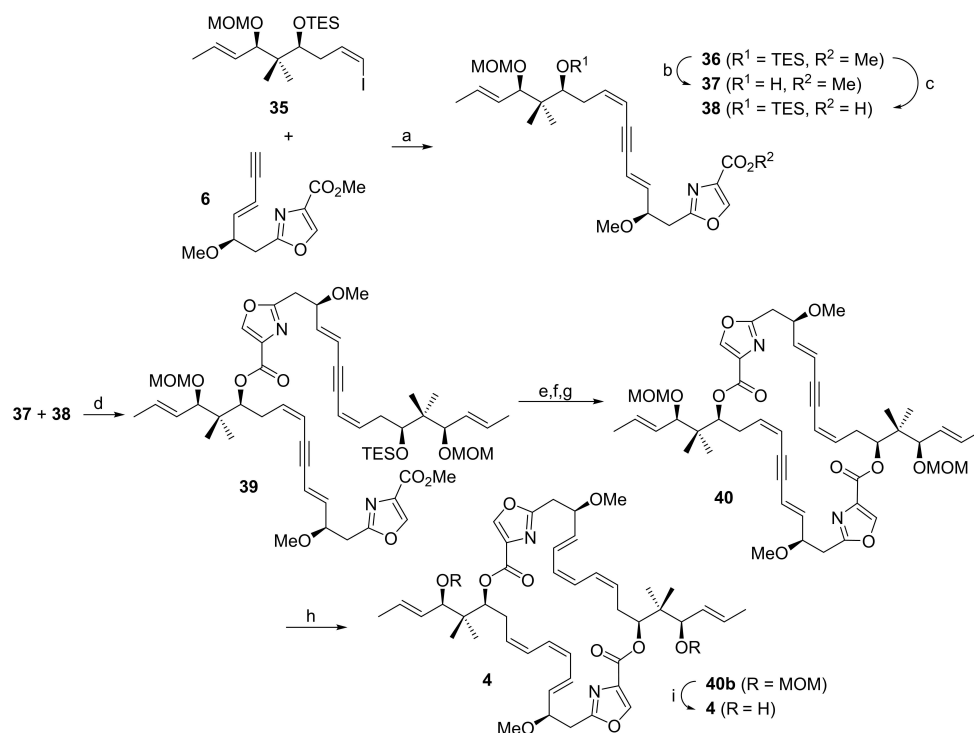
Conclusion

In conclusion, this work describes an application of our recently disclosed total synthesis of disorazole C₁ to the synthesis of three novel analogues, providing a reliable sequence for accessing numerous other derivatives of this highly active, naturally occurring molecule. In addition, the biological evaluation of the synthesized compounds extended the existing knowledge on the structure-activity relationships (SARs) of the disorazole family.

The potential for scale-up of the described synthesis may lead to the production of sufficient amount of material, which could finally result in the use of one of these molecules as payloads for antibody-drug conjugates (ADCs).

Experimental Section

The data and procedures that support the findings of this study are available in the Supporting Information.



Scheme 7. Total synthesis of analogue 4. Reagents and conditions: a) $\text{Pd}(\text{PPh}_3)_2\text{Cl}_2$, CuI , TEA , CH_3CN , -15°C to rt, 1 h, 85%; b) CSA , $\text{CH}_2\text{Cl}_2/\text{MeOH}$ 1:1, 0°C , 1 h, 95%; c) 1 M LiOH , THF , rt, 3 h, 99%; d) 1. TCBC , TEA , THF , rt, 2 h, 2. DMAP , $\text{THF}/\text{toluene}$, rt, 16 h, 75%; e) CSA , $\text{CH}_2\text{Cl}_2/\text{MeOH}$ 1:1, 0°C , 1 h; f) 1 M LiOH , THF , rt, overnight; g) 1. TCBC , TEA , THF , rt, 2 h, 2. DMAP , $\text{THF}/\text{toluene}$, rt, 16 h, 70% (3 steps); h) Zn (Ag/Cu), $\text{MeOH}/\text{H}_2\text{O}$ 1:1, 50°C , 24 h, 65%; i) HBr , $\text{CH}_3\text{CN}/\text{H}_2\text{O}$, 0°C , 1 h, 56%.

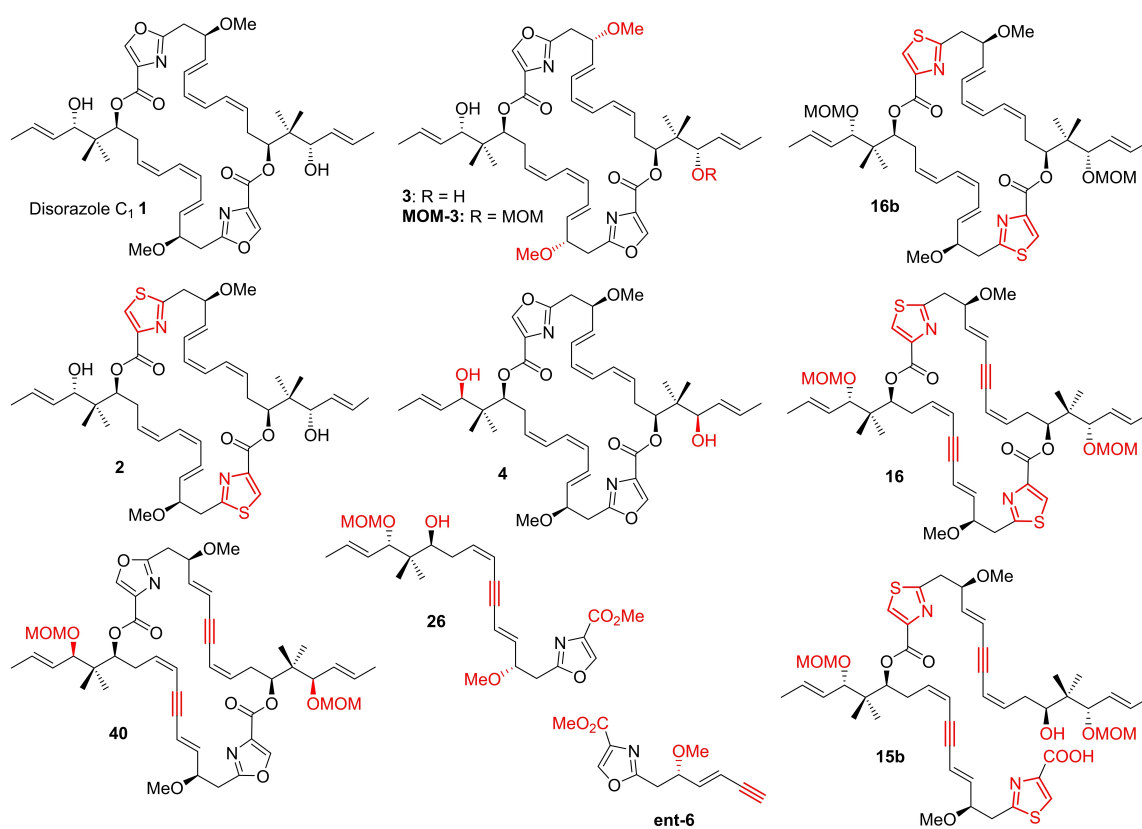


Figure 2. Structures of tested compounds. In red the differences with the natural product.

Table 1. Biological activities of disorazole C₁ and its analogues. Disorazole A₁ and epothilone B were used as internal standards. Abbreviations: n.a. = no activity; n.d. = not determined.

Cell line	KB3.1	A549	PC-3	MCF-7	SKOV-3	A431	
Mouse fibroblasts	Human cervix carcinoma	Human lung carcinoma	Human prostate carcinoma	Human breast adenocarcinoma	Human ovarian adenocarcinoma	Human squamous carcinoma	
Compound	IC ₅₀ (ng/mL)						
Epothilone B	0.24	0.017	0.034	0.048	0.015	n.d.	0.026
Disorazole A ₁	0.026	0.014	0.053	0.092	0.0015	0.023	n.d.
Disorazole C ₁	0.25	0.23	0.32	0.60	0.11	0.28	n.d.
Analogue 2	180	85	86	120	91	n.d.	82
Analogue 3	100	18	13	65	18	12	n.d.
Analogue 4	8600	7200	9000	7500	5400	n.d.	14000

Table 2. Biological activities of some intermediates. Disorazole A₁ and epothilone B were used as internal standards. Abbreviations: n.a. = no activity; n.d. = not determined.

Cell line	KB3.1	A549	PC-3	MCF-7	SKOV-3	A431	
L929 Mouse fibroblasts	Human cervix carcinoma	Human lung carcinoma	Human prostate carcinoma	Human breast adenocarcinoma	Human ovarian adenocarcinoma	Human squamous carcinoma	
Compound	IC ₅₀ (ng/mL)						
MOM-3	6800	4000	3700	4600	3500	4400	n.d.
16b	n.a.	2800	8300	1200	6300	n.d.	7000
16	n.a.	n.a.	n.d.	n.d.	n.d.	n.d.	n.d.
15b	n.a.	3300	13000	2900	3900	n.d.	4600
40	n.a.	11000	n.d.	n.d.	n.d.	n.d.	n.d.
26	n.a.	n.a.	n.d.	n.d.	n.d.	n.d.	n.d.
ent-6	n.a.	n.a.	n.d.	n.d.	n.d.	n.d.	n.d.

Acknowledgements

L.L. thanks the state of Saxony-Anhalt for a Ph.D. fellowship. Open Access funding enabled and organized by Projekt DEAL.

Conflict of Interest

The authors declare no conflict of interest.

Data Availability Statement

The data that support the findings of this study are available from the corresponding author upon reasonable request.

Keywords: analogues · biological evaluation · disorazoles · stereoselective · thiazole

- [1] R. Jansen, H. Irschik, H. Reichenbach, V. Wray, G. Hofle, *Liebigs Ann. Chem.* **1994**, 759–773.
- [2] H. Irschik, R. Jansen, F. Sasse, WO 2007/009897, **2007**.
- [3] Y. A. Elnakady, F. Sasse, H. Lünsdorf, H. Reichenbach, *Biochem. Pharmacol.* **2004**, *67*, 927–935.
- [4] M. B. Tierno, C. A. Kitchens, B. Petrik, T. H. Graham, P. Wipf, F. L. Xu, W. S. Saunders, B. S. Raccor, R. Balachandran, B. W. Day, J. R. Stout, C. E. Walczak, A. P. Ducruet, C. E. Reese, J. S. Lazo, *J. Pharmacol. Exp. Ther.* **2009**, *328*, 715–722.

- [5] F. L. Xu, Y. Rbaibi, K. Kiselyov, J. S. Lazo, P. Wipf, W. S. Saunders, *BMC Chem. Biol.* **2010**, *10*, 1.
- [6] L. Lizzadro, O. Spieß, D. Schinzer, *Org. Lett.* **2021**, *23*, 4543–4547.
- [7] W. Boland, N. Schroer, C. Sieler, M. Feigel, *Helv. Chim. Acta* **1987**, *70*, 102.
- [8] P. Wipf, T. H. Graham, J. Xiao, *Pure Appl. Chem.* **2007**, *79*, 753–761.
- [9] C. D. Hopkins, J. C. Schmitz, E. Chu, P. Wipf, *Org. Lett.* **2011**, *13*, 4088–4091.
- [10] R. Schäckel, B. Hinkelmann, F. Sasse, M. Kalesse, *Angew. Chem. Int. Ed.* **2010**, *49*, 1619–1622; *Angew. Chem.* **2010**, *122*, 1663–1666.
- [11] K. C. Nicolaou, M. Buchman, G. Bellavance, J. Krieger, P. Subramanian, K. K. Pulukuri, *J. Org. Chem.* **2018**, *83*, 12374–12389.
- [12] K. C. Nicolaou, J. Krieger, G. M. Murhade, P. Subramanian, B. D. Dherange, D. Vourloumis, S. Munneke, B. Lin, C. Gu, H. Sarvaia, J. Sandoval, Z. Zhang, M. Aujay, J. W. Purcell, J. Gavriluk, *J. Am. Chem. Soc.* **2020**, *142*, 15476–15487.
- [13] B. S. Pedersen, S. O. Lawesson, *Tetrahedron* **1979**, *35*, 2433–2437.
- [14] A. Hantzsch, J. H. Weber, *Ber. Dtsch. Chem. Ges.* **1887**, *20*, 3118.
- [15] C. H. Tan, A. B. Holmes, *Chem. Eur. J.* **2001**, *7*, 1845–1854.
- [16] J. A. Marshall, J. M. Salovich, B. G. Shearer, *J. Org. Chem.* **1990**, *55*, 2398–2403.
- [17] A. J. Phillips, Y. Uto, P. Wipf, M. J. Reno, D. R. Williams, *Org. Lett.* **2000**, *2*, 1165–1168.
- [18] K. Kubota, J. L. Leighton, *Angew. Chem. Int. Ed.* **2003**, *42*, 946–948; *Angew. Chem.* **2003**, *115*, 976–978.
- [19] S. D. Rychnovsky, B. Rogers, G. Yang, *J. Org. Chem.* **1993**, *58*, 3511–3515.
- [20] S. Hanessian, S. Giroux, A. Larsson, *Org. Lett.* **2006**, *8*, 5481–5484.
- [21] G. Stork, K. Zhao, *Tetrahedron Lett.* **1989**, *30*, 2173–2174.
- [22] For materials and methods refer to: a) L. Shao, Y. Marin-Felix, F. Surup, A. M. Stchigel, M. Stadler, *J. Fungi* **2020**, *6*, 188; b) K. Becker, A. C. Wessel, J. J. Luangsa-ard, M. Stadler, *Biomol. Eng.* **2020**, *10*, 805.

Manuscript received: August 8, 2022

Revised manuscript received: August 22, 2022

Accepted manuscript online: August 23, 2022

Version of record online: September 16, 2022